Astronomy Reports, Vol. 49, No. 3, 2005, pp. 217–225. Translated from Astronomicheskiĭ Zhurnal, Vol. 82, No. 3, 2005, pp. 247–255.

Atmospheric Elemental Abundances for the Components of the Multiple System ADS 11061. 41 Draconis

Yu. Yu. Balega[1], V. V. Leushin[1], and G. Weigelt[2]

[1]*Special Astrophysical Observatory, Russian Academy of Sciences, Nizhniĭ Arkhyz, Karachaĭ-Cherkessian Republic, 357147 Russia*

[2]*Max-Planck-Institut für Radioastronomie, Auf dem Hügel 69, Bonn, 53121 Germany*

Received March 25, 2004; in final form, September 20, 2004

Abstract—We obtained speckle interferometric and spectroscopic observations of the system 41 Dra during its periastron passage in 2001. The components' lines are resolved in the spectral interval 3700–9200 Å. The observed wavelength dependence of the brightness difference between the components is used to estimate the $B-V$ indices separately for each of the components: $B-V=0.511$ for component a and $B-V=0.502$ for component b. We derived improved effective temperatures of the components from their $B-V$ values and hydrogen-line profiles. The observations can be described with the parameters for the components $T^{\mathrm{a}}_{eff}=6370$ K, $\log g^{\mathrm{a}}=4.05$ and $T^{\mathrm{b}}_{eff}=6410$ K, $\log g^{\mathrm{b}}=4.20$. The iron, carbon, nitrogen, and oxygen abundances in the atmospheres of the components are $\log N(\mathrm{Fe})^{\mathrm{a}}=7.55$, $\log N(\mathrm{Fe})^{\mathrm{b}}=7.60$, $\log N(\mathrm{C})^{\mathrm{a}}=8.52$, $\log N(\mathrm{C})^{\mathrm{b}}=8.58$, $\log N(\mathrm{N})^{\mathrm{a}}=8.05$, $\log N(\mathrm{N})^{\mathrm{b}}=7.99$, $\log N(\mathrm{O})^{\mathrm{a}}=8.73$, $\log N(\mathrm{O})^{\mathrm{b}}=8.76$. *© 2005 Pleiades Publishing, Inc.*

1. INTRODUCTION

The quadruple system ADS 11061 contains two spectroscopic binaries, 40 Dra and 41 Dra, orbiting their common center of mass with a period of several tens of thousands of years and an apparent orbital semiaxis that varies from 10^3 to 10^4 AU [1]. The periods of the inner orbits of the 40 Dra and 41 Dra pairs are 10.5 and 1246.7 days [2]. The system is hierarchical and probably dynamically stable. All its components have spectral types of F5–F7. The iron abundance estimate of [3] indicates that ADS 11061 belongs to the young disk population, and that its age does not exceed 2.5 billion years. In late evolutionary stages, such stars become giants with luminosities only slightly different from those of the main-sequence stars.

The system is of special interest due to the very high orbital eccentricity of the 41 Dra pair: $e=0.9754\pm0.0001$ [2]. Their motion has been studied using both spectroscopic and interferometric methods, and the combined orbit's parameters are accurately known. For example, despite the system's long period, the epoch of periastron passage is known to within about 10 minutes. At periastron, the components of the pair approach each other to a distance of about 10 stellar radii. The high eccentricity raises the question of how such a pair could be formed and why its orbit has not been circularized by the action of tidal forces over the system's lifetime, as has happened for 40 Dra. One possible scenario of the origin and dynamic evolution of ADS 11061 was suggested in [2], but the situation is far from completely clear. In the recent periastron passage of 41 Dra in May–June 2001, it was possible to obtain integrated spectra in which the components' spectra were fully resolved during a comparatively short time interval (±15 days from periastron). This made it possible to obtain reliable information on the atmospheric chemical compositions of each of the stars.

Analyses of the orbit of the 41 Dra pair yielded the components' masses, $M^{\mathrm{a}}=(1.39\pm0.15)M_\odot$ and $M^{\mathrm{b}}=(1.30\pm0.14)M_\odot$, and the system's dynamic parallax [2]. An accurate parallax is crucial for determining the star's luminosity and, provided the temperatures are known, the components' radii. Essentially all estimates of π are close to $\pi=0.023''$ [1–6], whereas the parallax of 41 Dra in the HIPPARCOS catalog is $0.01884''$ [7], much lower than this value. The HIPPARCOS value is probably wrong, since the measurements did not take into account the system's binarity. Thus, the probable distance to the system is 44.6 ± 1.0 pc.

Below, we present the results of our estimates of the components' temperatures and of the iron, carbon, nitrogen, and oxygen abundances in their atmospheres based on spectra taken with the echelle spectrographs of the 6 m and Zeiss-1000 telescopes

Table 1. Brightness differences between the components of 41 Dra

λ, Å/$\Delta\lambda$, Å	$\Delta m \pm$ uncertainty	Date
5000	$0.40^m \pm 0.04^m$	2001.2713
5450/300	0.48 ± 0.03	1998.7769
6000	0.46 ± 0.05	2001.2713
6050/240	0.20 ± 0.10	1993.3492
6050/240	0.30 ± 0.10	1993.7646
6050/240	0.30 ± 0.10	1993.8437
6560/300	0.38 ± 0.05	1994.7129
7000	0.44 ± 0.10	2001.2713
8500/300	0.41 ± 0.14	2001.2713
12390/1380	0.47 ± 0.20	2000.7800
12390/1380	0.55 ± 0.20	2001.1920
16480/3170	0.46 ± 0.20	2000.7800
21910/4110	0.47 ± 0.10	1996.2667

of the Special Astrophysical Observatory (Russian Academy of Sciences) and the Zeiss-2000 telescope of the International Center for Astronomical, Medical, and Ecological Research (Mt. Terskol) [8–11]. The spectrographs have resolutions from 15 000 to 100 000 and cover the spectral range from 3700 Å to 9200 Å. We also analyze the brightness differences of the components of 41 Dra estimated over a wide wavelength range via speckle interferometry and compare these to the spectroscopic data.

2. EFFECTIVE TEMPERATURES OF THE COMPONENTS OF 41 DRA

Earlier [12], we determined the effective temperatures of the system's components from the continuum spectral energy distribution of the system [13] and the equivalent widths and profiles of the observed hydrogen lines. However, we noted certain discrepancies in the data. Thus, these earlier results need to be verified and refined. For this purpose, we use color indices in the UBV system, estimates of the brightness differences of the components obtained from speckle interferometry, and ratios of line depths in the components' spectra measured when the lines for the two components can be resolved.

Though the $B-V$ values for 41 Dra in various catalogs [14, 15] differ slightly, it is reasonable to adopt the combined color index for the system $B-V = 0.507 \pm 0.001$.

We noted in [12] that the speckle-interferometric brightness difference between the components was, on average, $\Delta m = 0.426 \pm 0.028$. However, it is very important to find the wavelength dependence of this difference in order to determine the individual color indices and temperatures of the components. For this purpose, we collected all the speckle-interferometric estimates of Δm obtained with the 6-m telescope, shown in Table 1. These lead to the following wavelength dependence for Δm:

$$\Delta m = 0.330 + 0.863 \times 10^{-5}\,[\text{Å}^{-1}] \times \lambda\,[\text{Å}].$$

This means that, at the center of the B band ($\lambda 4400$ Å), $\Delta m^{\rm B} = 0.368$, and at the center of the V band ($\lambda 5500$ Å), $\Delta m^{\rm V} = 0.377$.

We measured the ratios of the central depths of unblended lines of the system's components using spectra covering the wavelength range from 3700 to 9200 Å obtained at phases close to periastron. The central depths of absorption lines in the combined spectrum of the system are related to the components' luminosities as

$$\frac{R^{{\rm a},obs}}{R^{{\rm b},obs}} = \frac{E^{\rm a}_\lambda}{E^{\rm b}_\lambda}\frac{R^{\rm a}}{R^{\rm b}},$$

where $R^{\rm a}$, $R^{\rm b}$ and $R^{{\rm a},obs}$, $R^{{\rm b},obs}$ are the actual and observed central line depths, respectively. If the physical characteristics and chemical compositions of the components are similar, then

$$R^{\rm a} \approx R^{\rm b} \quad \text{and} \quad E^{\rm b}/E^{\rm a} = R^{{\rm b},obs}/R^{{\rm a},obs}.$$

Our measurements of some 300 lines show that these ratios are wavelength-dependent:

$$E^{\rm b}_\lambda/E^{\rm a}_\lambda = 0.73 - 0.54 \times 10^{-5}\,[\text{Å}^{-1}] \times \lambda\,[\text{Å}].$$

Transforming the luminosity ratios into magnitude differences, we obtain

$$\Delta m^{{\rm B},obs} = 0.378 \pm 0.008$$
$$\text{and} \;\; \Delta m^{{\rm V},obs} = 0.387 \pm 0.008,$$

in fairly close agreement with the speckle-interferometric Δm estimates.

The assumption that the B and V magnitudes for the system's components are related as

$$B^{\rm b} = B^{\rm a} + \Delta m^{{\rm B},obs} \;\; \text{and} \;\; V^{\rm b} = V^{\rm a} + \Delta m^{{\rm V},obs}$$

is a good approximation. In this case, the system's observed $B-V$ color index will be

$$B - V = (B^{\rm a} - V^{\rm a}) - 2.5\log\frac{1+10^{-0.4\Delta m^{{\rm B},obs}}}{1+10^{-0.4\Delta m^{{\rm V},obs}}},$$

and $B^{\rm b} - V^{\rm b} = B^{\rm a} - V^{\rm a} + (\Delta m^{{\rm B},obs} - \Delta m^{{\rm V},obs})$.

Substituting the observed values into these relations, we can derive the color indices for each of the components in the 41 Dra system:

component a: $B - V = B^{\rm a} - V^{\rm a} = 0.511$,

component b: $B - V = B^{\rm b} - V^{\rm b} = 0.502$.

Using models with normal chemical composition and an atmospheric turbulent velocity of 2 km/s of Kurucz [16], we obtain for the components' effective temperatures

component a: $T^{\mathrm{a}}_{eff} = 6370 \pm 20$ K,

component b: $T^{\mathrm{b}}_{eff} = 6410 \pm 20$ K.

These temperatures are slightly lower than those we derived in [12], and close to the estimates of T_{eff} and $B - V$ obtained from evolutionary tracks [2].

Using the masses and luminosities derived from the orbital motion, the parallax presented in [2], and our T_{eff} estimates, we find the components' surface gravities to be

component a: $\log g^{\mathrm{a}} = 4.05 \pm 0.10$,

component b: $\log g^{\mathrm{b}} = 4.20 \pm 0.10$.

3. RADIAL VELOCITIES OF THE COMPONENTS OF 46 DRA

To model the system's spectra and compare the synthesized spectra with observations at various orbital phases, we must obtain measurements of the components' radial velocities. We used stellar lines near Hα, using Earth-atmospheric lines as a comparison spectrum. A list of the measured lines is presented in Table 2.

Table 2. Lines used to measure the components' radial velocities

Stellar lines		Atmospheric lines
6526.653 SiI	6575.037 FeI	6532.359 H_2O
6546.239 FeI	6583.710 SiI	6536.720 H_2O
6554.223 TiI	6586.308 NiI	6542.313 H_2O
6555.463 SiI	6587.610 C I	6547.705 H_2O
6559.588 TiII	6592.926 FeI	6548.622 H_2O
6562.808 Hα	6593.884 FeI	6552.629 H_2O
6569.216 FeI	6597.571 FeI	6557.171 H_2O
6571.174 FeI	6604.600 ScII	6572.086 H_2O
6572.779 CaI	6608.044 FeI	6574.852 H_2O
6574.228 FeI	6609.118 FeI	6599.324 H_2O

We calculated the radial velocities and reduced them to the Sun using the Dech20 code of Galazutdinov [17]. The measured radial velocities of the components relative to the Earth, V^{a}_r and V^{b}_r, are presented in Table 3, together with the correction to the Sun V_a. The phases were calculated with the elements $T =$ JD 2449571.037 and $P = 1246.680^{\mathrm{d}}$.

The derived radial velocities are in good agreement with those of [2], confirming the correctness of the orbital elements of 41 Dra presented in that paper.

4. HYDROGEN LINE PROFILES

Synthetic spectra of 41 Dra near Hα were calculated by summing theoretical profiles derived using the SintVa code developed by Tsimbal [18]. We calculated the theoretical profiles using models with $T_{eff} = 6370$ K and $\log g = 4.05$ for component a and $T_{eff} = 6410$ K and $\log g = 4.20$ for component b. The models were derived by interpolating the model grid of Kurucz [16]. The combined synthetic Hα spectrum was calculated for four phases before and after the periastron passage in 2001. We used the components' radial velocities from Table 3 to take into account wavelength shifts in the observed spectrum. The rotational speeds of the components ($v \sin i$) needed to calculate the synthetic spectrum were determined from absorption lines of metals. The rotational speeds of both components are close to 8.5 km/s. The turbulent velocities in the components' atmospheres were determined in [3] to be $V^{\mathrm{a}}_t = 2.15$ km/s and $V^{\mathrm{b}}_t = 1.70$ km/s. When summing the spectra, we assumed a brightness ratio for the components of $E^{\mathrm{b}}/E^{\mathrm{a}} = 0.68$.

The figure shows a comparison of the calculated and observed profiles, together with theoretical profiles we calculated for a binary whose components both have $T_{eff} = 6500$ K and $\log g = 4.00$, with the same brightness ratios, turbulent velocities, and radial velocities as for the first version. At all phases, the observed Hα profiles are confined within the range of the theoretical results. However, the agreement with the model having $T_{eff} = 6370$ K and $\log g = 4.05$ for component a and $T_{eff} = 6410$ K and $\log g = 4.20$ for component b is appreciably better. This confirms the correctness of our choice of atmospheric parameters for the components of the 41 Dra system.

5. ATMOSPHERIC IRON ABUNDANCES OF THE COMPONENTS OF 41 DRA

We determined the iron abundances from the equivalent widths of 50 FeI lines and 38 FeII lines using spectra taken near periastron, when the lines of components a and b were clearly resolved. The equivalent widths of these lines, along with the atomic parameters and $\log N(\mathrm{Fe})$ values for each line and at various phases, are presented in [3], where we also describe the technique used to determine $\log N(\mathrm{Fe})$. The calculations were performed with the KONTUR code [19]. Using models with $T_{eff} = 6575$ and $\log g = 4.08$ for component a and $T_{eff} = 6600$ and $\log g = 4.26$ for component b yielded

Table 3. Radial velocities of the components of 41 Dra

Spectrum	Date	JD	Phase	$V_r^{\rm a}$, km/s	$V_r^{\rm b}$, km/s	V_a, km/s
z3818	14.11.2000	2451862.6090	0.8381	11.86 ± 1.52	1.85 ± 1.12	4.27
z3819	14.11.2000	2451862.6924	0.8382	11.13 ± 1.32	1.92 ± 1.32	4.28
t05311	20.01.2001	2451929.6299	0.8916	13.89 ± 1.67	-2.15 ± 1.22	−3.45
t05312	20.01.2001	2451929.6715	0.8917	13.54 ± 1.77	-2.07 ± 1.35	−3.46
t05413	21.01.2001	2451930.5882	0.8924	14.12 ± 1.85	-2.43 ± 1.56	−3.55
o05a	09.06.2001	2452070.4215	0.0046	-27.12 ± 1.09	44.85 ± 1.38	−1.33
t11406	26.11.2027	2452605.4215	0.4337	5.92 ± 1.37	5.48 ± 1.37	2.94

$\log N(\mathrm{Fe}) = 7.66$ (component a) and $\log N(\mathrm{Fe}) = 7.72$ (component b), which are slightly higher than the solar iron abundance ($\log N(\mathrm{Fe})_\odot = 7.50$). This paper's refined effective temperatures and surface gravities for the components ($T^{\rm a}_{eff} = 6370$ K and $\log g^{\rm a} = 4.05$, $T^{\rm b}_{eff} = 6410$ K and $\log g^{\rm b} = 4.20$) lead to abundances much closer to the solar value.

The lines of neutral iron, FeI, gave the atmospheric abundances for the components

component a: $\log N(\mathrm{Fe}) = 7.582 \pm 0.044$,

component b: $\log N(\mathrm{Fe}) = 7.593 \pm 0.032$.

The abundances derived from lines of ionized iron, FeII, are

component a: $\log N(\mathrm{Fe}) = 7.530 \pm 0.039$,

component b: $\log N(\mathrm{Fe}) = 7.613 \pm 0.045$.

The rms errors of the average values describe the internal uncertainties of the results, which coincide within the errors. Thus, the system's iron overabundance relative to the Sun, if present, does not exceed +0.1dex.

Note that any further decrease in the effective temperatures for the model atmospheres would lead to poorer coincidence of the $\log N(\mathrm{Fe})$ values derived from ions with different ionization stages. For a model temperature of 6100 K, the difference in the iron abundances derived for component a from the FeI and FeII lines is 0.13dex, and that for component b is 0.27dex, which are much larger than the uncertainties. Thus, we consider our atmospheric parameters to be confirmed by the ionization relations.

6. ATMOSPHERIC CARBON, NITROGEN, AND OXYGEN ABUNDANCES OF THE COMPONENTS OF 46 DRA

The abundances of carbon, nitrogen, and oxygen are largely determined by the evolutionary status of the star, and are an important source of information about the star's origin and history. The amount of carbon and nitrogen in stars more massive than the Sun determines the rate of hydrogen-burning nuclear reactions in the CN cycle, and thus the rate of the star's evolution. In addition, carbon, nitrogen, and oxygen, the most abundant elements in normal stars heavier than hydrogen and helium, determine the internal structure of the atmosphere and of the star as a whole. At the same time, the comparative poorness of these elements' line spectra introduces considerable difficulties in determining their abundances. For this reason, the vast majority of papers analyzing C, N, and O abundances in stellar atmospheres are based on measurements of one or two lines of each element in the stellar spectra. This makes it important to measure each carbon, nitrogen, and oxygen line present in the spectrum in order to more accurately derive the abundances. Correctly taking into account the physical conditions under which the analyzed spectral lines are formed is also important.

Our echelle spectra (3700–9200 Å) were acquired near the periastron passage, when the components' spectral lines were resolved, enabling us to identify and measure relatively many CI, NI, and OI lines in the spectrum of each of the system's components.

Table 4 presents the parameters of the CI lines measured in the spectrum of the 41 Dra system, together with the equivalent widths, W_λ (in mÅ), and carbon abundances, $\log N(\mathrm{C})$, for each of the components. We determined W_λ for each of the components from the $W_\lambda^{{\rm a},obs}$ and $W_\lambda^{{\rm b},obs}$ values measured for the resolved lines assuming the brightness ratio $l = E^{\rm b}/E^{\rm a} = 0.68$. The actual equivalent widths in the spectra of the components are given by the relations $W_\lambda^{\rm a} = 1.68 W_\lambda^{{\rm a},obs}$ and $W_\lambda^{\rm b} = 2.50 W_\lambda^{{\rm b},obs}$.

The model atmospheres and the techniques used to derive the abundances were the same as those used in our analysis of the iron lines. The $\log gf$ values were mainly taken from the VALD list [20].

Table 4. Line parameters, CI equivalent widths, and carbon abundances in the atmospheres of components a and b of 41 DRA

λ, Å	ε_i, eV	$\log gf$	W_λ^a, mÅ	$\log N(C)^a$	W_λ^b, mÅ	$\log N(C)^b$
4762.31	7.48	−2.46	15.4	8.51	15.6	8.51
4762.53	7.48	−2.34	16.6	8.37	17.1	8.38
4792.66	7.95	−2.79	8	8.71	8	8.70
4815.22	7.95	−2.13	7.4	8.00	8	8.03
4815.48	7.95	−2.42	8.2	8.52	8.2	8.51
4817.37	7.48	−3.04	8.4	8.65	11	8.74
4926.43	8.54	−1.97	6.8	8.55	7.5	8.55
4932.05	7.68	−1.88	59.4	8.89	55.5	8.64
5039.05	7.95	−1.79	19.7	8.23	23	8.37
5039.10	7.95	−2.29	10	8.51	11	8.52
5040.12	7.95	−2.3	7	8.23	10.5	8.52
5052.17	7.68	−1.65	59	8.69	63.5	8.76
5380.34	7.68	−1.84	49.2	8.72	40	8.59
5515.55	8.85	−2.34	2.9	8.76	2.9	8.76
5793.12	7.95	−2.06	18.4	8.56	24	8.66
5800.60	7.95	−2.34	8.7	8.50	12	8.59
6586.27	9.00	−1.89	3.8	8.53	3.2	8.52
6587.61	8.54	−1.6	17.4	8.55	18.4	8.57
6588.64	9.17	−2.2	1.9	8.71	1.8	8.68
6591.46	8.85	−2.41	3	8.69	3.5	8.72
6595.24	8.85	−2.41	2.8	8.67	2.5	8.64
6602.41	8.85	−2.38	5	8.83	3.2	8.68
6605.78	8.85	−2.31	1.1	8.51	1.2	8.38
6611.35	8.85	−1.84	2.5	7.97	3.2	8.12
7116.99	8.65	−0.91	40	8.48	42	8.52
7119.66	8.64	−1.15	31.9	8.55	35	8.60
7132.11	8.65	−2.2	3.4	8.53	7	8.67
9061.43	7.48	−0.35	214	8.69	224	8.82
9062.49	7.48	−0.46	185.4	8.58	195.4	8.72
9078.29	7.48	−0.58	160.4	8.48	187.4	8.76
9088.52	7.48	−0.43	167.5	8.40	177.5	8.56
9094.83	7.49	0.15	218	8.26	228	8.44
9111.80	7.49	−0.3	184.9	8.45	225	8.78

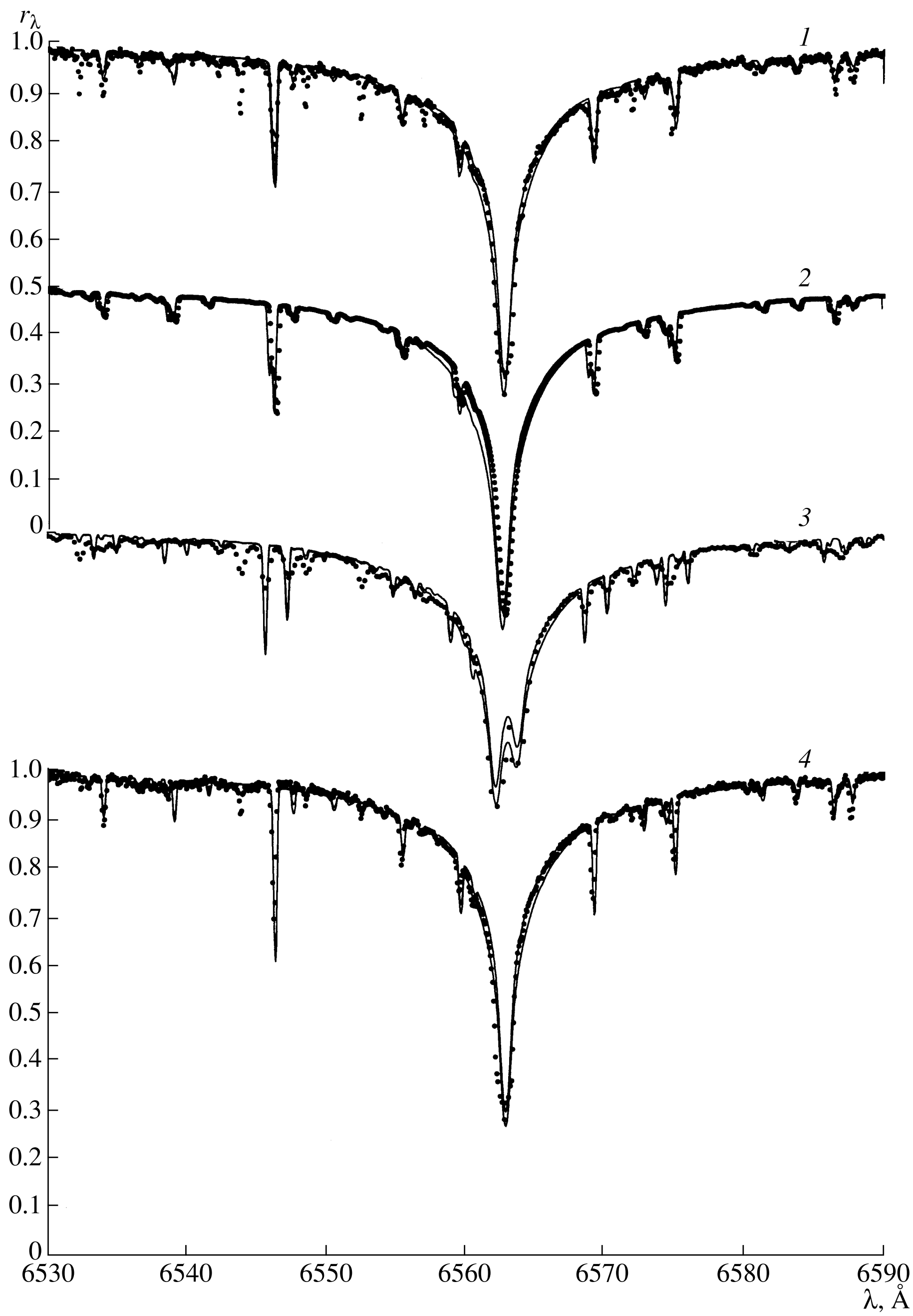

Comparison of observed (dots) and synthetic (solid curves) spectra of 41 Dra. The upper theoretical spectrum was calculated for $T_{eff}^{\rm a} = 6370$ K, $\log g^{\rm a} = 4.05$ and $T_{eff}^{\rm b} = 6410$ K, $\log g^{\rm b} = 4.20$. The lower theoretical spectrum was calculated for $T_{eff} = 6500$ K and $\log g = 4.00$. The spectra correspond to phases (*1*) 0.83, (*2*) 0.89, (*3*) 0.00, (*4*) 0.43.

Our equivalent-width calculations included four broadening mechanisms for the absorption coefficient: radiation damping, Doppler broadening, broadening due to the quadratic Stark effect, and van der Waals broadening. These effects enter the absorption coefficient as:

$$a = (\Delta\lambda_R + \Delta\lambda_{st} + \Delta\lambda_w)/\Delta\lambda_D,$$
$$v = (\Delta\lambda + d)/\Delta\lambda_D,$$

where $\Delta\lambda_R$ is the line width due to radiation damping, $\Delta\lambda_{st}$ is the Stark width, $\Delta\lambda_w$ is the van der Waals width, and d is the Stark displacement.

$\Delta\lambda_w$ can be calculated using the approximate formula of Unsold:

$$\Delta\lambda_w = \lambda^2/(4\pi c)\mathrm{C}_6^{0.4} \times 34N(\mathrm{HeI})(8kT/\pi m_H)^{0.3}.$$

Table 5. Line parameters, NI equivalent widths, and nitrogen abundances in the atmospheres of components a and b

λ, Å	ε_i, eV	$\log gf$	W_λ^{a}, mÅ	$\log N(\mathrm{N})^{\mathrm{a}}$	W_λ^{b}, mÅ	$\log N(\mathrm{N})^{\mathrm{b}}$
4253.39	10.34	−1.37	7.5	8.66	2	7.99
7442.30	10.33	−0.38	9.4	7.98	10	8.00
8184.86	10.33	−0.29	7.6	7.87	5.8	7.60
8188.01	10.32	−0.29	16.8	8.15	23	8.35
8216.33	10.34	0.13	21.2	7.92	16	7.66
8680.28	10.34	0.35	30.9	7.93	38.2	8.06
8683.40	10.33	0.09	26.5	8.04	28.5	8.07
8686.15	10.33	−0.3	19.6	8.17	23.8	8.29
8703.25	10.33	−0.32	8.4	7.85	8.5	7.80
8711.71	10.33	−0.23	16.1	8.02	12.5	7.92
8718.83	10.34	−0.34	11.2	7.97	18.5	8.17

Table 6. Line parameters, OI equivalent widths, and oxygen abundances in the atmospheres of components a and b

λ, Å	ε_i, eV	$\log gf$	W_λ^{a}, mÅ	$\log N(\mathrm{O})^{\mathrm{a}}$	W_λ^{b}, mÅ	$\log N(\mathrm{O})^{\mathrm{b}}$
6155.96	10.74	−1.36	1.9	8.83	2.4	8.86
6155.97	10.74	−1.01	3.6	8.78	4.8	8.83
6155.98	10.74	−1.12	3	8.80	3.8	8.84
6156.74	10.74	−1.49	1.5	8.84	1.7	8.84
6156.76	10.74	−0.9	4.6	8.78	5.2	8.80
6156.78	10.74	−0.69	6.3	8.75	7.1	8.76
6158.14	10.74	−1.84	1	8.91	–	–
6158.18	10.74	−1.00	4.9	8.85	–	–
6158.19	10.74	−0.41	11.6	8.77	–	–
7771.94	9.15	0.37	143.6	9.02	131.6	8.97
7774.16	9.15	0.22	123.3	8.93	117.6	8.94
7775.39	9.15	0.00	99.1	8.85	90.5	8.81
8446.25	9.52	−0.46	35.1	8.46	42.7	8.69
8446.36	9.52	0.24	51.7	8.09	63	8.31
8446.76	9.52	0.01	48	8.24	58.5	8.46

Here, line broadening due to collisions with neutral hydrogen and helium atoms is taken into account, and the constant C_6 can either be fixed (we took it from the VALD list) or calculated as

$$C_6 = 6.5 \times 10^{-9}((Z+1)^2 + 13.595)/\chi_{up})^{4/5},$$

where Z is the ion's charge and χ_{up} is the ionization potential for the upper level.

We used two techniques to take into account the quadratic Stark effect. For lines for which accurate calculations are available, we can specify the temperature-dependent electron-collision half-width, w, the ion-collision half-width, α, and the displacement, d [21]. The Stark line width and displacement can then be calculated for any point in the atmosphere using the equations

$$\Delta\lambda_{st} = 2wN_e \times 10^{-16}(1 + \alpha N_e^{1/4} A),$$

$$d = wN_e \times 10^{-16}(d/w + \alpha N_e^{1/4} B),$$

where $A = 1.75(1 - 0.75r)$, $B = 2(1 - 0.75r)$ for neutral atoms; $A = 1.75(1 - 1.2r)$, $B = 2(1 - 1.2r)$

for ions; and $r = 1.85\pi^{1/6} N_e^{1/6} (e^2/kT)^{1/2}$ is the Debye shielding radius.

If no data for w, α, and d are available, we use the following approximation to estimate the Stark broadening:

$$\Delta\lambda_{st} = \lambda^2/(4\pi c) \mathrm{C}_4 N_e,$$

where the constant C_4 is taken from the VALD list or calculated as

$$\mathrm{C}_4 = 10^{-8} \times ((Z+1)^2 + 13.595)/\chi_{up})^{5/2}.$$

The mean carbon abundances derived for the atmospheres of components a and b via a comparison of the observed and calculated equivalent widths are

component a: $\log N(\mathrm{C}) = 8.524 \pm 0.036$,

component b: $\log N(\mathrm{C}) = 8.576 \pm 0.031$.

There are many fewer nitrogen lines than carbon lines in the spectra of 41 Dra, and nearly all measurable lines that are not blended with lines of other elements have $\lambda > 8000$ Å. We could find only two NI lines in the shorter-wavelength part of the spectrum: λ4253.39 Å and λ7442.30 Å, which have equivalent widths lower than 10 mÅ. Table 5 collects for the NI lines the same data as those shown in Table 4 for the carbon lines. The mean atmospheric nitrogen abundances of components a and b are

component a: $\log N(\mathrm{N}) = 8.051 \pm 0.068$,

component b: $\log N(\mathrm{N}) = 7.991 \pm 0.034$.

We determined the atmospheric abundances of oxygen for the components of 41 Dra from lines of five triplets in the red, beginning with $\lambda > 6100$ Å. The parameters of the measured lines and $\log N(\mathrm{O})$ values for both components are presented in Table 6. The lines are fairly strong and essentially unblended, ensuring the reliability of our oxygen abundance determinations. The atmospheric abundances for each of the components are

component a: $\log N(\mathrm{O}) = 8.727 \pm 0.067$,

component b: $\log N(\mathrm{O}) = 8.761 \pm 0.055$.

7. CONCLUSION

Our spectroscopic and speckle-interferometric observations of the binary system 41 Dra in the hierarchical multiple system ADS 11061 obtained close to its periastron passage have enabled us to study the atmospheres of each of the components of 41 Dra separately. Within the uncertainties, all our observational data indicate that the effective temperatures of the system's components are 6370 K and 6410 K, respectively, for components a and b.

The virtually exact coincidence of the elemental abundances studied for the atmospheres of the two components of 41 Dra with those in the solar atmosphere and meteorites [22] is remarkable; the differences of several hundredths of a dex are probably due to equivalent-width errors and are not significant. This may mean that the chemical composition of the interstellar medium within a 50 pc radius of the Sun did not experience any considerable changes during the time from the formation of the solar system some five billion years ago until the formation of the 41 Dra system 2.5 billion years ago [2]. At the same time, the absence of any significant deviations of the C : N : O ratios in the atmospheres of the 41 Dra components from the solar values testify to a complete absence of mixing between the core and the atmosphere, despite the shock gravitational stresses periodically experienced by the stars during their periastron passages, when they approach each other to distances of only a few stellar radii.

ACKNOWLEDGMENTS

The authors thanks F.A. Musaev and D.O. Kudryavtsev for taking the spectra of 41 Dra. This study was supported by the Russian Foundation for Basic Research (project no. 01-02-16563-a).

REFERENCES

1. A. A. Kisilev and L. G. Romanenko, Astron. Zh. **73**, 875 (1996) [Astron. Rep. **40**, 795 (1996)].
2. A. Tokovinin, Yu. Yu. Balega, E. A. Pluzhnik, *et al.*, Astron. Astrophys. **409**, 245 (2003).
3. Yu. Yu. Balega, V. V. Leushin, and G. Weigelt, Bull. Spec. Astrophys. Obs. **54**, 5 (2003).
4. A. Tokovinin, Pis'ma Astron. Zh. **21**, 286 (1995) [Astron. Lett. **21**, 250 (1995)].
5. I. I. Balega, Yu. Yu. Balega, G. Fal'ke, *et al.*, Pis'ma Astron. Zh. **23**, 774 (1997) [Astron. Lett. **23**, 172 (1997)].
6. V. A. Al-Wardat, Yu. Yu. Balega, V. V. Leushin, *et al.*, *IAU Symp. No. 210: Modelling of Stellar Atmospheres, June 17–21, 2002, Uppsala, Sweden.*
7. *The Hypparcos and Tycho Catalogues*. ESA SP-1200, ESA, 1997.
8. F. A. Musaev, Pis'ma Astron. Zh. **19**, 776 (1993) [Astron. Lett. **19**, 315 (1993)].
9. V. E. Panchuk, I. D. Najdenov, V. G. Klochkova, *et al.*, Bull. Spec. Astrophys. Obs. **44**, 127 (1998).
10. V. E. Panchuk and S. V. Ermakov, Spets. Astrofiz. Obs., Nauchno-Tekh. Otchet No. 267 (1999).
11. F. A. Musaev, G. A. Galazutdinov, A. V. Sergeev, *et al.*, Kinematika Fiz. Nebesnykh Tel **15**, 282 (1999).
12. Yu. Yu. Balega, V. V. Leushin, and E. A. Pluzhnik, Bull. Spec. Astrophys. Observ. **51**, 61 (2001).
13. A. V. Kharitonov, V. M. Tereshchenko, and L. N. Knyazeva, *Spectrophotometric Catalogue of Stars* (Nauka, Alma-Ata, 1988).
14. H. L. Johnson and W. W. Morgan, Astrophys. J. **117**, 313 (1953).

15. V. G. Kornilov, I. M. Volkov, A. I. Zakharov, *et al.*, *Catalogue UBVR of Northern Sky Bright Stars* (Tr. Gos. Astron. Inst. Shternberga, Moscow, 1991), Vol. 63.
16. R. Kurucz, http://kurucz.harvard.edu
17. G. A. Galazutdinov, Preprint No. 92, SAO (Spec. Astrophys. Obs., 1992).
18. V. V. Tsimbal, *Magnetic Stars* (Spec. Astrophys. Obs., Russ. Acad. Sci., Nizhniĭ Arkhyz, 2003) (in press).
19. V. V. Leushin and G. P. Topil'skaya, Astrofiz. **22**, 121 (1985) [Astrophys. **21**, 74 (1985)].
20. F. Kupka, N. E. Piskunov, T. A. Ryabchikova, *et al.*, Astron. Astrophys., Suppl. Ser. **138**, 119 (1999).
21. G. Grim, *Spectral Line Widening in Plasma* (Mir, Moscow, 1978).
22. N. Grevesse and A. J. Sauval, *Solar Composition and Its Evolution—From Core to Corona*, Ed. by C. Frolich, M. C. E. Huber, S. K. Solanki, and R. von Steiger (Kluwer, Dordrecht, 1998), p. 161.

Translated by N. Samus'